Available online at www.sciencedirect.com
ScienceDirect
Materials Research Bulletin 42 (2007) 851–860
Materials Research Bulletin
www.elsevier.com/locate/matresbu

Thermal stability of the Mobil Five type metallosilicate molecular sieves—An in situ high temperature X-ray diffraction study

D.S. Bhange, Veda Ramaswamy *

Catalysis Division, National Chemical Laboratory, Pune-411004, India

Received 1 February 2006; received in revised form 10 August 2006; accepted 25 August 2006
Available online 18 September 2006

Abstract

We have carried out in situ high temperature X-ray diffraction (HTXRD) studies of silicalite-1 (S-1) and metallosilicate molecular sieves containing iron, titanium and zirconium having Mobil Five (MFI) structure (iron silicalite-1 (FeS-1), titanium silicalite-1 (TS-1) and zirconium silicalite-1 (ZrS-1), respectively) in order to study the thermal stability of these materials. Isomorphous substitution of Si^{4+} by metal atoms is confirmed by the expansion of unit cell volume by X-ray diffraction (XRD) and the presence of Si–O–M stretching band at $\sim$960 cm^{-1} by Fourier transform infrared (FTIR) spectroscopy. Appearance of cristobalite phase is seen at 1023 and 1173 K in S-1 and FeS-1 samples. While the samples S-1 and FeS-1 decompose completely to cristobalite at 1173 and 1323 K, respectively, the other two samples are thermally stable upto 1623 K. This transformation is irreversible. Although all materials show a negative lattice thermal expansion, their lattice thermal expansion coefficients vary. The thermal expansion behavior in all samples is anisotropic with relative strength of contraction along '*a*' axes is more than along '*b*' and '*c*' axes in S-1, TS-1, ZrS-1 and vice versa in FeS-1. Lattice thermal expansion coefficients (α_v) in the temperature range 298–1023 K were -6.75×10^{-6} K^{-1} for S-1, -12.91×10^{-6} K^{-1} for FeS-1, -16.02×10^{-6} K^{-1} for TS-1 and -17.92×10^{-6} K^{-1} for ZrS-1. The highest lattice thermal expansion coefficients (α_v) obtained were -11.53×10^{-6} K^{-1} for FeS-1 in temperature range 298–1173 K, -20.86×10^{-6} K^{-1} for TS-1 and -25.54×10^{-6} K^{-1} for ZrS-1, respectively, in the temperature range 298–1623 K. Tetravalent cation substitution for Si^{4+} in the lattice leads to a high thermal stability as compared to substitution by trivalent cations.

Keywords: A. Microporous materials; C. X-ray diffraction; D. Thermal expansion

1. Introduction

Zeolites are open, crystalline inorganic materials with ordered pore structures. Mobil Five (MFI) type molecular sieves have two-dimensional (2D) connected channel system [1]. These channels are made up of 10 membered rings. The two types of channels present are elliptical 10-ring straight channel along the *b* axis with free cross section of 5.7–5.8 Å × 5.1–5.2 Å and nearly circular 10-ring sinusoidal channel along the *a* axis with free cross section of 5.4 ± 0.2 Å as shown in Fig. 1. Due to this structural architecture, MFI-type of materials shows tremendous impact as shape selective industrial catalysts. These types of molecular sieves have potential use in separation of some gases and

* Corresponding author. Tel.: +91 20 2590 2012; fax: +91 20 2590 2633.
E-mail address: v.ramaswamy@ncl.res.in (V. Ramaswamy).

0025-5408/$ – see front matter
doi:10.1016/j.materresbull.2006.08.024

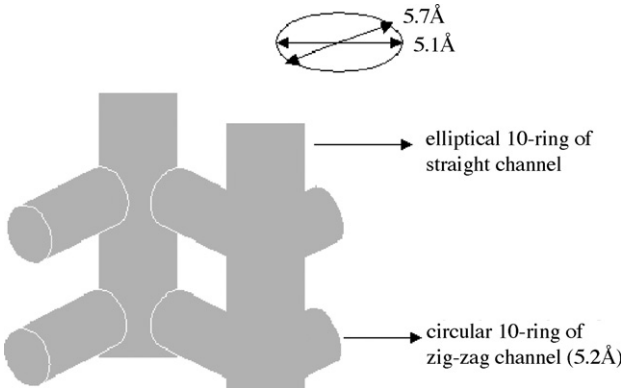

Fig. 1. Schematic presentation of channels in MFI molecular sieves.

liquids, which is very difficult by conventional means. The isomorphous substitution of Si^{4+} ions by other tetrahedrally coordinated elements such as Al [1], B [2], Ti [3], Ga [4], Fe [5], Zr [6] and Mn [7] in small amounts (1–2.5 wt%) have opened a new class of compounds which shows specific catalytic properties in alkylation, isomerisation, oxidation and hydroxylation reactions. These catalytic properties are due to the tunable oxidation and/or coordination states of heteroatoms in the framework. TS-1 is a highly selective and active heterogeneous oxidation catalyst for the epoxidation of olefins and hydroxylation of phenol and linear alkanes [8]. Fe silicalite-1 is a known catalyst for benzene hydroxylation [9], ethyl benzene to styrene [10] and NO_x reduction [11] reactions. Many of the vapor phase reactions are carried out at more than 623 K and catalysts are activated at more than 773 K. During activation of the catalysts the temperature may go upto 1023 K. Thus, these materials used as catalysts need to have the appropriate thermal and hydrothermal stability to withstand the extreme conditions frequently involved in their use and regeneration. Thus, the information regarding the stability of these materials is necessary. Zeolites are metastable. Their stability are different in different environments viz., acidic or alkaline. They are also stable to ionizing radiation and can be used to adsorb radioactive cations. The reports on manganese silicalite-1 (MnS-1) [7] aluminophosphate-17 ($AlPO_4$-17) [12] and ZrS-1 [13] molecular sieves are the few studies done by in situ high temperature X-ray diffraction (HTXRD) measurements. Upon heating, zeolites undergo different kinds of structural changes including: (i) cell volume contraction due to the removal of water and/or templating organic molecules (dehydration and calcination); (ii) displacive or reconstructive phase transformation(s) to more or less metastable phase(s); (iii) structural collapse; (iv) structural breakdown (i.e. complete amorphization); (v) negative thermal expansion (NTE).

In the present work, an in situ HTXRD technique is employed to study the stability of siliceous MFI and metallosilicates such as iron silicalite-1 (FeS-1), titanium silicalite-1 (TS-1) and zirconium silicalite-1 (ZrS-1). Since the thermal behavior of trivalent cations is more unstable than the tetravalent cation substituted zeolites, the in situ HTXRD work has been carried out in different temperature ranges.

2. Experimental

2.1. Materials used

Sodium silicate (27.6% SiO_2), tetrapropylammonium hydroxide (TPAOH) (Aldrich, 20% aqueous), concentrated sulphuric acid H_2SO_4, iron nitrate [$Fe(NO_3)_3.\cdot 9H_2O$], tetraethyl orthosilicate (TEOS) (Aldrich, 98%), zirconium chloride ($ZrCl_4$) (Merck, 99%) and titanium isopropoxide [$Ti(iPrO)_4$] were used for the synthesis of silicalite-1 and metallosilicates molecular sieves (S-1, FeS-1, TS-1 and ZrS-1).

2.2. Synthesis

Silicalite-1 and metalosilicate molecular sieves were prepared by hydrothermal synthesis. Silicalite-1 (siliceous anologue of MFI) and Fe-silicalite-1 (Si/Fe = 50) were synthesized by the procedure reported by Szostak and Thomas [5]. In a typical synthesis of S-1, 50 g of Na-silicate (27% SiO_2) was dissolved in 50 g of distilled water and to this

4.5 g concentrated H_2SO_4 was added dropwise. Six grams of TPAOH in 10 ml water was added to above solution and resulting gel was stirred for 30 min and transferred to Teflon lined autoclave. Synthesis of FeS-1 (Si/Fe = 50) was carried out similarly by adding 1.818 g $Fe(NO_3)_3{\cdot}9H_2O$ before addition of template to avoid precipitation of Fe. Synthesis of TS-1 (Si/Ti = 50) was carried out according to the procedure patented by Taramasso et al. [3]. ZrS-1 (Si/Zr = 50) used in the present work was prepared by the method published elsewhere [6]. All the syntheses were carried out in Teflon lined stainless steel autoclave under autogenous pressure. The crystallization was carried out at 433 K for 48 h, under static conditions. After the crystallization, the solid products were filtered, washed with deionized water, dried at 383 K and designated as 'as synthesized' samples which contains the template TPAOH. These samples were calcined in air at 823 K for 16 h and further treated with 1 M ammonium acetate solution to remove alkali metal impurities, if any and are further calcined at 773 K in air for 8 h and designated as calcined samples.

2.3. Characterization

Powder X-ray diffraction (PXRD) patterns of as synthesized as well as calcined S-1, FeS-1, TS-1 and ZrS-1 samples were collected on a Philips X' Pert Pro 3040/60 diffractometer using Cu Kα radiation (λ = 1.5418 Å), nickel filter and an X'celerator as detector which employs the RTMS (Real Time Multiple Strip) detection technique. PXRD patterns were collected in the 2θ range 5–60° with steps of 0.017°, using continuous scanning mode, the scan time per step was 50 s.

Scanning electron micrographs (SEM) of the samples were recorded on a JOEL-JSM-5200 scanning electron microscope to observe the morphology of the oxide particles. Energy dispersive analysis of X-rays (EDAX) measurements were performed on a Leica Stereoscan-440, Scanning electron microscope equipped with a Phoenix EDAX attachment. The framework infrared (IR) spectra of the samples were recorded on potassium bromide (KBr) pellet in the mid framework region (1100–400 cm^{-1}) using a Shimadzu model 8300 Fourier transform infrared (FTIR) spectrometer. Thermal analysis was done on a Setaram thermal analyzer (SETARAM) at a heating rate of 10 °C min^{-1} in air atmosphere.

2.4. In situ HTXRD

Calcined samples S-1, FeS-1 TS-1 and ZrS-1 were subjected to in situ high temperature powder XRD experiments to observe the structural stability of the sample as a function of temperature. The high temperature powder XRD data were recorded on a Philips X'Pert Pro 3040/60 XRD unit equipped with Anton Paar HTK 1600 attachment. Alumina was used as the standard for calibration of the high temperature stage. A small amount of sample was mounted on a platinum strip, which serves as the sample stage as well as the heating element. A Pt/Rh–13% thermocouple spot-welded to the bottom of the stage was used for measuring the temperature. The HTXRD patterns were scanned in the 2θ range 5–55° with a step size of 0.02° and a rate of 1° min^{-1} for S-1 and ZrS-1 samples using Ni-filtered Cu Kα radiations (λ = 1.54187 Å). While the HTXRD patterns were scanned for TS-1 and FeS-1 samples, in the 2θ range 5–60° with a step size of 0.02° and a rate of 1° min^{-1} using Fe-filtered Co Kα (λ = 1.7903 Å) radiation. Scintillation counter was the detector employed for the data collection of all the samples. The patterns were scanned between range 298 K (room temperature) and 1623 K in static air. The powder patterns were recorded at temperature intervals of 150 K from 423 to 1623 K. A heating rate of 10 K min^{-1} and a soaking time of 10 min were employed. The XRD profiles were refined using X'pert plus refining package provided by Philips to obtain information on the lattice parameters and the phase composition.

3. Results and discussion

Both as synthesized and calcined S-1, FeS-1, TS-1 and ZrS-1 samples were white powders exhibiting the typical X-ray diffraction pattern of microporous and highly crystalline molecular sieves with the MFI topology (Fig. 2a and b, respectively). No typical diffraction peaks due to metal oxide aggregates were found. In as synthesized samples, the intensities were less for reflections 1 0 1, 0 1 1 and 2 0 0 due to asymmetry in pore, i.e. presence of template. Progress in intensities of these reflections has been observed after calcination (Fig. 2b). All the materials have shown orthorhombic symmetry except calcined S-1, which shows monoclinic symmetry. Lattice parameters of all these materials were obtained by Rietveld refinement and used for calculating the negative thermal expansion. Values for

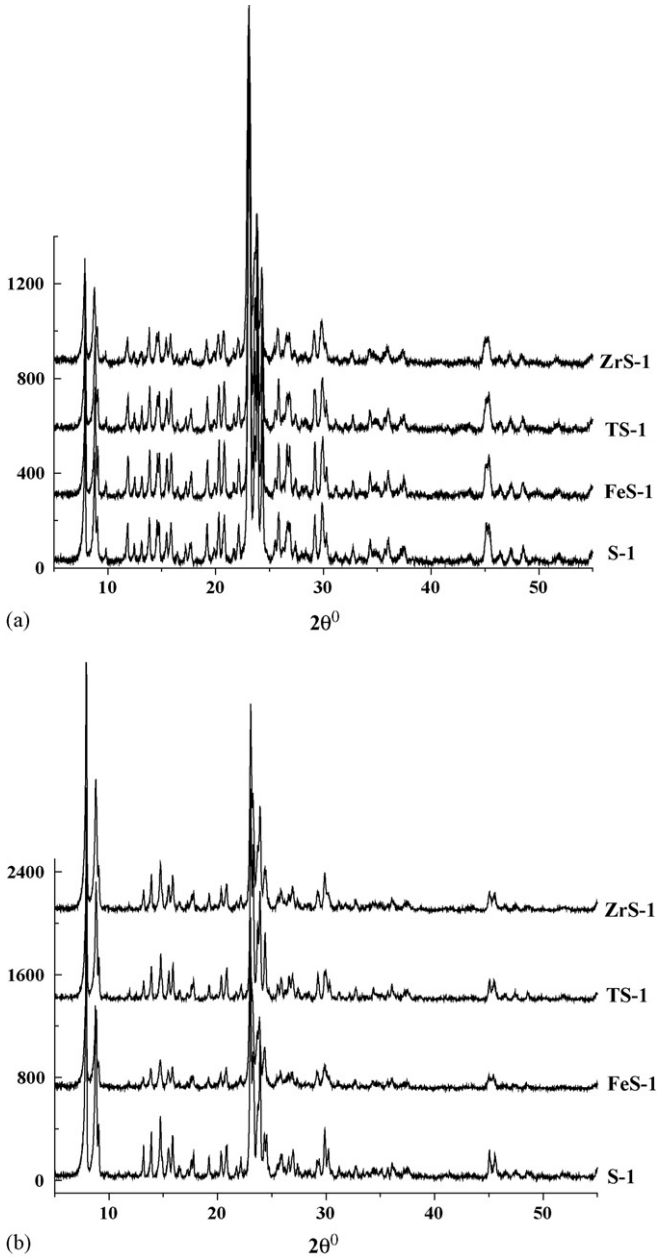

Fig. 2. (a) Powder XRD patterns of as synthesized materials S-1, FeS-1, TS-1 and ZrS-1 samples and (b) Powder XRD patterns of calcined materials S-1, FeS-1, TS-1 and ZrS-1 samples.

unit cell volume parameters at room temperature are given in Table 1. It can be seen that there is an expansion in unit cell of FeS-1, TS-1 and ZrS-1 which is due to the isomorphous substitution of Si^{4+} by the higher ionic radii hetero metal atom Fe^{3+}, Ti^{4+} and Zr^{4+}, respectively, in the framework of MFI structure. The theoretical unit cell volume calculated using the ionic radii of the cations, from the formula $V_x = V_{Sil} - V_{Sil}[1 - (M–O)^3/(Si–O)^3]x$ where V_{Sil} and V_x are the unit cell volume of the silicalite-1 and sample with x wt% of metal ion substituted, respectively, M–O is the bond distance of the metal ion substituted, x is the wt% of the metal ion in the samples, are also given in the Table 1. Comparing the calculated and experimental unit cell volume, it can be seen that approximately 73, 53 and 9% of Fe, Ti and Zr are isomorphously substituted into the silicalite framework. In the case of FeS-1, although the ionic radii of

Table 1
Lattice parameter and framework density of S-1, FeS-1, TS-1 and ZrS-1 at room temperature

Sample	Lattice parameters						FD/1000 (Å)^3
	a (Å)	b (Å)	c (Å)	β (°)	V (Å)^3 Observed	V^a (Å)^3 Calculated	
S-1	20.120	19.880	13.370	90.57	5347.76	5348	17.95
FeS-1	20.083	19.976	13.428	90	5387.42	5401	17.82
TS-1	20.102	19.912	13.409	90	5367.02	5384	17.88
ZrS-1	20.094	19.897	13.394	90	5355.44	5429	17.93

FD, framework density.
[a] Metal–oxygen (M–O) bond distances for S-1, FeS-1, TS-1 and ZrS-1 were taken as 1.87, 2.10, 2.03 and 2.20 Å, respectively.

Fe^{3+} (0.49 Å) is higher than Ti^{4+} (0.42 Å), higher concentration of Fe^{3+} is incorporated in the lattice than the latter due to the flexibility of the framework by the interaction of the charge compensating cations. Zr being still a bigger cation (r = 0.59 Å) than Fe, could be incorporated at smaller concentration in the lattice, although the input concentration of all the cations are the same.

Fig. 3 shows the SEM of the samples, which was magnified 10^4 times. It shows that S-1 particles were prismatic and not aggregated. The size of the S-1 crystals (~1 μm) differed from the other samples. The FeS-1 and TS-1 particles were prismatic and aggregated. The ZrS-1 particles were spherical, well dispersed and were not aggregated unlike FeS-1 and TS-1. Particle size of the metallosilicate molecular sieve is <1 μm. The silicon to metal ratio determined by

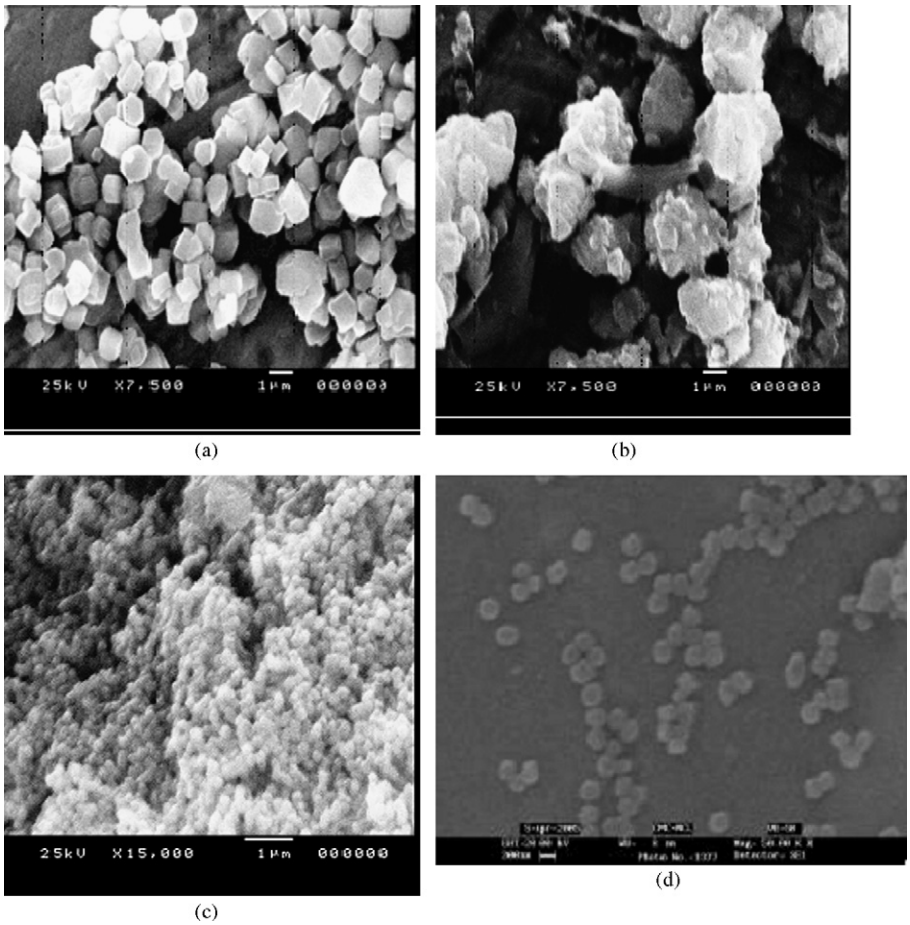

Fig. 3. Scanning electron micrographs of calcined samples of (a) S-1, (b) FeS-1, (c) TS-1 and (d) ZrS-1.

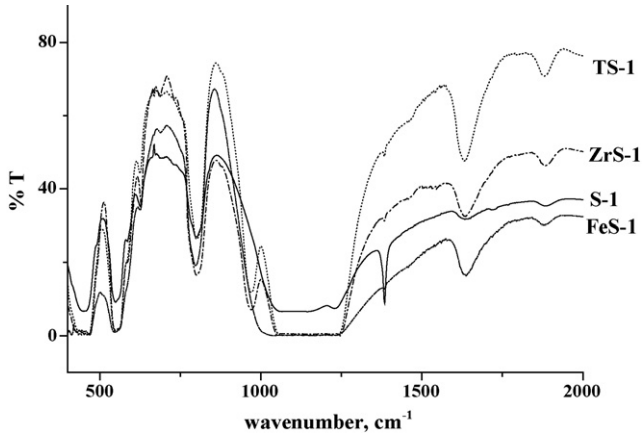

Fig. 4. IR spectra of calcined S-1, FeS-1, TS-1 and ZrS-1 samples using KBr.

EDAX are Si/Fe = 49 for FeS-1, Si/Zr = 50 for ZrS-1 and Si/Ti = 53 for TS-1 samples. This indicates the presence the hetero metal atoms in the respective metallosilicate molecular sieves.

The FTIR spectra of all the samples are shown in Fig. 4. A band at $\sim$960 cm^{-1} is attributed to the stretching vibrations of SiO_4 tetrahedron bound to heteroatoms as Si–O–M linkages [14]. In TS-1 and ZrS-1, this band is visible clearly but in the case of FeS-1 there is a broadening [5] in that region indicating the substitution of hetero metal atom in the silicate lattice framework.

Multiple plot of HTXRD pattern as a function of temperature for S-1 is shown in Fig. 5. Appearance of cristobalite phase is seen in the HTXRD profile at 1023 K and the structure of S-1 collapses completely at 1173 K. More details are reported earlier [13] on the effect of temperature on the unit cell parameters in S-1 sample. Fig. 6 shows the HTXRD

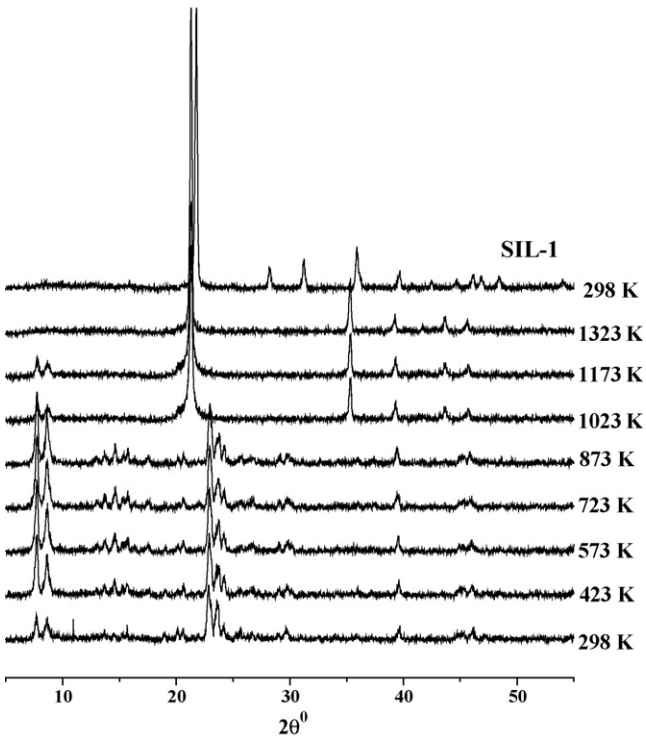

Fig. 5. Multiple plot of powder XRD patterns of calcined S-1 sample scanned in air at various temperatures from 298 to 1323 K at 150 K intervals and at 298 K after cooling.

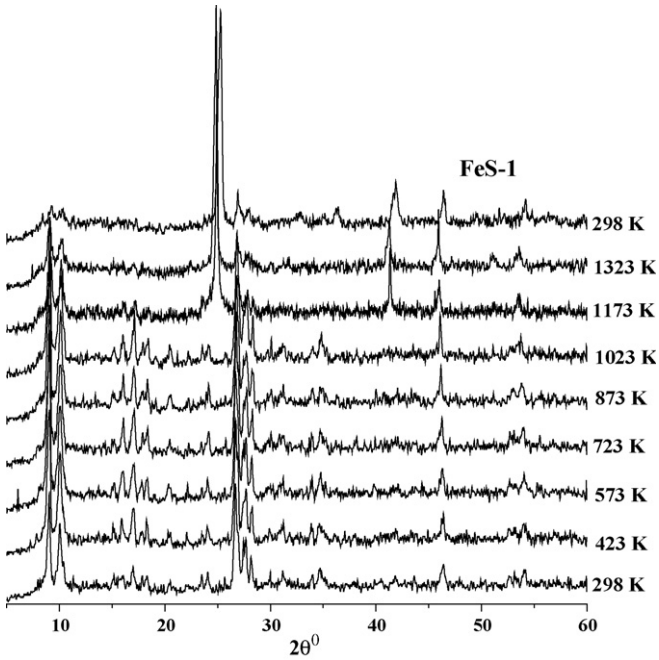

Fig. 6. Multiple plot of powder XRD patterns of calcined FeS-1 sample scanned in air at various temperatures from 298 to 1323 K at 150 K intervals and at 298 K after cooling.

profiles of FeS-1 from 298 to 1323 K and after cooling to room temperature. Cristobalite phase is seen at 1173 K and the MFI structure decomposed to cristobalite (SiO_2) at 1323 K. In the case of tetravalent metallosilicate analogues, TS-1 and ZrS-1, the material is stable up to 1623 K. The multiple plots as a function of temperature for TS-1 and ZrS-1 are shown in Figs. 7 and 8, respectively. The crystallinity of all the samples does not vary with temperature. Siliceous zeolites have higher thermal stability provided they have no defects in the framework structure [15]. Petrovic et al. [16]

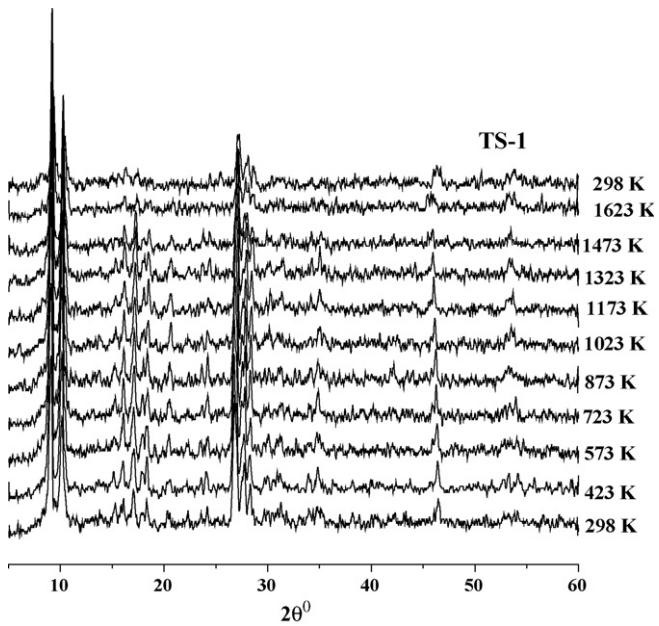

Fig. 7. Multiple plot of powder XRD patterns of calcined TS-1 sample scanned in air at various temperatures from 298 to 1623 K at 150 K intervals and at 298 K after cooling.

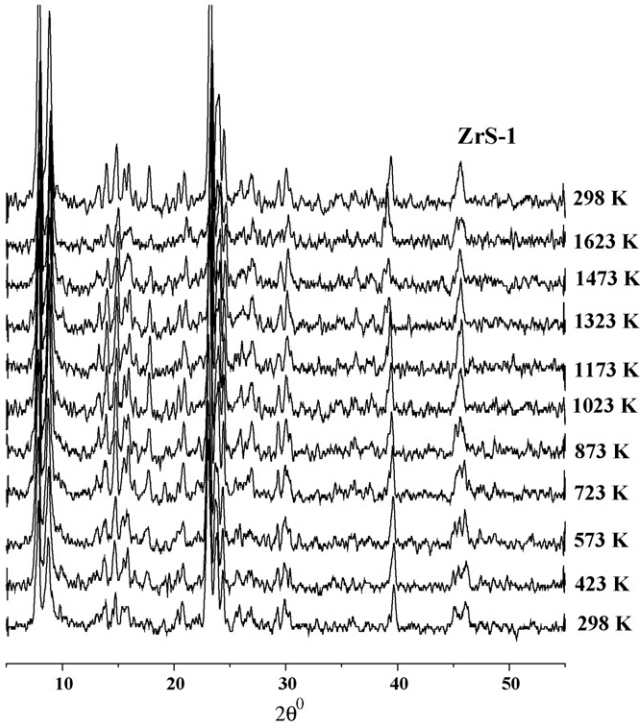

Fig. 8. Multiple plot of powder XRD patterns of calcined ZrS-1 sample scanned in air at various temperatures from 298 to 1623 K at 150 K intervals and at 298 K after cooling.

have carried out detailed thermochemical studies of the stability of frameworks in high silica zeolites ZSM-5, ZSM-11, ZSM-12, SSZ-24 and faujasite to correlate the crystal structure with stability. They have reported that a Si–O–Si angle below 140° is the major destabilizing factor. de Boer et al. [17] also show that a linear relationship between the destabilization and the percentages of angles smaller than or equal to 140° in the structure does not exist for a large number of structures. Since we could not do the refinement of the HTXRD profiles (which are scanned fast and the counting statistics are not good), we could not calculate the bond angles in S-1 and FeS-1 to correlate the Si–O–Si bond angles with the destabilization. The thermal contraction in the framework structure is likely to induce a decrease in T–O–T angles with increase of temperature. The destabilizing factor or the thermally weaker silicalite-1 at 1023 K is likely due to the defects in the framework and also due to the distortion of the tetrahedra in its flexible framework and its anharmonic vibrations resulting in shortening of the bonds. S-1 and FeS-1 decomposes to cristobalite which is the stable phase having six membered rings in its framework. In the case of FeS-1, the lower charge of Fe^{3+} requires charge compensation thereby producing lattice strain sufficient to promote decomposition of that material at 1173 K. On the other hand, in the case of TS-1 and ZrS-1, the flexibility of the framework for the isomorphous substitution of Si^{4+} by the larger cation Ti^{4+} and Zr^{4+} is depending on the composition of the cations and the framework density.

Flexibility of zeolite framework is to some extent, revealed by the possible variation in the framework density of the structure, which depends on the composition and pore volume. The framework density calculated using the unit cell volume (from XRD data) of the four samples is given in Table 1. The data in Table 1 reveal that the flexibility of FeS-1 is less than the corresponding Ti and Zr analogues (reflected in framework density value). Subtle difference in electrostatic and covalent bond interactions in FeS-1 lowers the thermal stability as compared to the covalent interactions in TS-1 and ZrS-1. van Santen and co-workers have extensively studied the lattice relaxation of silica [18] and $AlPO_4$ polymorphs [19] and have reported the relative importance of the electrostatic versus covalent interactions in structural stability. Comparison of volume thermal expansion coefficients and framework density of FeS-1, TS-1 and ZrS-1 (Fig. 9) with respect to temperatures shows that the strength of contraction increases with the increase in

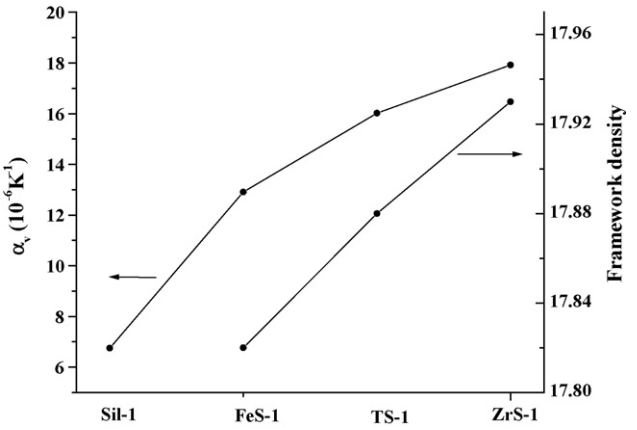

Fig. 9. Variation of framework density with volume thermal expansion coefficient in S-1, FeS-1, TS-1 and ZrS-1 samples.

framework density. Higher the framework density of the metallosilicate molecular sieves having MFI structure higher is the stability. The effect of 'T' atoms (T = Fe, Ti and Zr) on the thermal stability can thus be correlated to the framework density determined experimentally.

According to Lightfoot and co-workers [20], Si–O–Si/M bond angle is responsible for negative thermal expansion (NTE) in zeolite systems. Transverse vibrations of these bonds give rise to negative thermal expansion of materials. Table 2 gives the lattice/volume thermal expansion coefficient (TEC) of S-1, FeS-1, TS-1 and ZrS-1 samples. Lattice or volume thermal expansion coefficient was calculated using the formula, $\alpha_v = \Delta V/(T - RT)V_{RT}$ where T and RT are the typical temperature of the scan and room temperature, respectively, ΔV is the difference in the unit cell volume of the material at T and RT. NTE is anisotropic in all the materials, it is more along 'a' and 'c' axes than 'b' axis in TS-1 and ZrS-1 and it is more along 'b' and 'c' than 'a' axes in FeS-1. Lattice thermal expansion coefficients (α_v) in temperature range 298–1023 K were -6.75×10^{-6} K^{-1} for S-1, -12.91×10^{-6} K^{-1} for FeS-1, -16.02×10^{-6} K^{-1} for TS-1 and -17.92×10^{-6} K^{-1} for ZrS-1. Isomorphous substitution of Si^{4+} by Fe^{3+}, Ti^{4+} and Zr^{4+} in the framework has increased the thermal stability of the material with respect to S-1 and the strength of NTE is increased to two to three times (Table 2). The highest lattice thermal expansion coefficient (α_v) was -11.53×10^{-6} K^{-1} for FeS-1, in the temperature range 298–1173 K, -20.86×10^{-6} K^{-1} for TS-1 and -25.54×10^{-6} K^{-1} for ZrS-1, respectively, in the temperature range 298–1623 K. The difference in the magnitude of NTE is likely due to the composition and nature of heteroatom present in the lattice. The coefficient of negative thermal expansion decreases in this order, ZrS-1 > TS-1 > FeS-1 > S-1. The very strong NTE coefficients observed is likely due to the transverse vibration of the bridging oxygen in two-fold coordination between two polyhedrons causing a shortening of Si–Si non-bonding distance [21,22].

Due to the low torsional and bending frequencies of the [T–O–T] bond, the zeolite lattice is highly flexible. When the topology of the zeolite framework requires the adaptation of bond lengths and bond angles, T–O–T angle and bond length changes are more preferred over deformation of the tetrahedra [19]. In our heteroatom substituted samples, FeS-1 is less stable than the other two samples. It is seen from the unit cell expansion in Table 1 that ~73% of Fe whose

Table 2
Thermal expansion coefficients of S-1, FeS-1, TS-1 and ZrS-1 for different temperature ranges

Sample	Thermal expansion coefficient ($\times 10^{-6}$ K^{-1})					
	α_a 298–1023 K	α_b 298–1023 K	α_c 298–1023 K	α_v 298–1023 K	α_v 298–1173 K	α_v 298–1623 K
S-1	−5.758	−0.485	−0.619	−6.75	[a]	[a]
FeS-1	−2.765	−4.720	−5.544	−12.91	−11.53	[a]
TS-1	−7.328	−3.740	−5.040	−16.02	−17.81	−20.86
ZrS-1	−8.237	−4.50	−5.251	−17.92	−18.88	−25.54

[a] Structure collapsed.

bond length is ∼1.84 Å, is incorporated into the tetrahedral silicalite-1 framework, whereas only 53% of Ti (Ti–O = 1.77 Å) is isomorphously substituted and the rest is due to the extra framework Fe or Ti as the case may be. Zr being a bigger ion with Zr–O = 1.94 Å, showed a lower expansion on substitution, due to the distorted tetrahedral symmetry of the Zr cation which is already reported that there is the presence of tetrahedrally coordinated, isolated Zr sites with Si–O–Zr linkages in ZrS-1 and ZrS-2 samples [23,24].

4. Conclusions

In situ high temperature X-ray diffraction (HTXRD) studies on silicalite-1 and metallosilicate molecular sieves (FeS-1, TS-1 and ZrS-1) with MFI structure (Si/M = 50) were carried out to study thermal behavior in the temperature range 298–1623 K. The structure of S-1 and FeS-1 collapsed at 1173 and 1323 K, respectively. The monoclinic and orthorhombic phase of S-1 and FeS-1, respectively, transformed to α-cristobalite. The structure of TS-1 and ZrS-1 were stable even upto 1623 K. The thermal behavior of trivalent and tetravalent cations in the MFI framework depends on the role of counter cation present in the former. The sharp negative thermal expansion seen in all the samples is anisotropic, with relative strength of contraction in '*a*' axis is being greater than '*b*' and '*c*' axes in TS-1 and ZrS-1 while contraction is less along '*a*' axis in FeS-1. Lattice thermal expansion coefficients (α_v) in the temperature range 298–1023 K were $-6.75 \times 10^{-6}\,K^{-1}$ for S-1, $-12.91 \times 10^{-6}\,K^{-1}$ for FeS-1, $-16.02 \times 10^{-6}\,K^{-1}$ for TS-1 and $-17.92 \times 10^{-6}\,K^{-1}$ for ZrS-1. The highest lattice thermal expansion coefficients (α_v) obtained were $-11.53 \times 10^{-6}\,K^{-1}$ for FeS-1 in temperature range 298–1173 K, $-20.86 \times 10^{-6}\,K^{-1}$ for TS-1 and $-25.54 \times 10^{-6}\,K^{-1}$ for ZrS-1, respectively, in the temperature range 298–1623 K. The strength of contraction increases with increase in framework density in the three-metallosilicate molecular sieves studied. Lower framework density of FeS-1 is responsible for its low thermal stability. While tetravalent cation substituted metallosilicate molecular sieves show very high thermal stability, trivalent cation substituted samples are structurally/thermally less stable.

Acknowledgement

One of the authors (D.S.B.) thanks University Grant Commission, New Delhi, India, for a Research Fellowship.

References

[1] E.M. Flanigen, J.M. Bennett, R.W. Grose, J.P. Cohen, R.L. Patton, R.M. Krichner, J.V. Smith, Nature 271 (1978) 512.
[2] G. Coudurier, A.J. Auroux, C. Vedrine, R.D. Farlee, L. Abrams, R.D. Shannon, J. Catal. 108 (1987) 1.
[3] M. Taramasso, G. Perego, B. Notari, US Patent No. 4,410,501 (1983).
[4] C.R. Bayese, A.P.R. Kentgens, J.W. de Haan, L.J.M. van de Ven, Phys. Chem. 96 (1992) 755.
[5] R. Szostak, T.L. Thomas, J. Catal. 100 (1986) 555.
[6] B. Rakshe, V. Ramaswamy, S.G. Hegde, R. Vetrivel, A.V. Ramaswamy, Catal. Lett. 45 (1997) 41.
[7] N.N. Tusar, N.Z. Logar, I. Arcon, F. Thibault-Starzyk, A. Ristic, N. Rajic, V. Kaucic, Chem. Mater. 15 (2003) 4745.
[8] B. Notari, Adv. Catal. 41 (1996) 253.
[9] A.S. Kharitonov, V.B. Fenelonov, T.P. Voskresenskaya, N.A. Rudina, V.V. Molchanov, L.M. Plyasova, G.I. Panov, Zeolites 15 (1995) 253.
[10] G. Vorbeck, M. Richter, R. Fricke, B. Parlitz, E. Screier, K. Szulmewsky, B. Zibrowius, Stud. Surf. Sci. Catal. 65 (1991) 631.
[11] V.I. Sobolev, G.I. Panov, A.S. Kharitonov, V.N. Rommanikov, A.M. Volodin, K.G. Ione, J. Catal. 139 (1993) 435.
[12] M.P. Attfield, A.W. Sleight, Chem. Mater. 1 (1998) 2013.
[13] D.S. Bhange, V. Ramaswamy, Mater. Res. Bull. 41 (2006) 1392.
[14] A. Thangaraj, R. Kumar, S.P. Mirajkar, P. Ratnasamy, J. Catal. 130 (1991) 1.
[15] G. Niu, Y. Huang, X. Chen, J. He, Y. Liu, A. He, Appl. Catal. B: Environ. 21 (1999) 63.
[16] I. Petrovic, A. Navrotsky, M.E. Davis, S.I. Zones, Chem. Mater. 5 (1993) 1805.
[17] K. de Boer, A.P.J. Jansen, R.A. van Santen, Phys. Rev. 52 (1995) 12579.
[18] G.J. Kramer, B.W.H. van Beest, R.A. van Santen, Nature 351 (1991) 636.
[19] R.A. van Santen, A.J.M. de Man, W.P.J.H. Jacobs, E.H. Teunissen, G.J. Kramer, Catal. Lett. 9 (1991) 273.
[20] D.A. Woodcock, P. Lightfoot, L.A. Villaescusa, M.J. Diaz Cabanas, M.A. Camblor, Chem. Mater. 11 (1999) 2508.
[21] V. Korthuis, N. Khosrovani, A.W. Sleight, N. Roberts, R. Dupree, W.W. Warren, Chem. Mater. 7 (1995) 412.
[22] A.W. Sleight, Endeavor 19 (1995) 64.
[23] B. Rakshe, V. Ramaswamy, A.V. Ramaswamy, J. Catal. 163 (1995) 412.
[24] V. Ramaswamy, B. Tripathi, D. Srinivas, A.V. Ramaswamy, R. Cattaneo, R. Prins, J. Catal. 200 (2001) 250.